Spatial and Spatio-temporal Epidemiology 25 (2018) 57–66

Contents lists available at ScienceDirect

Spatial and Spatio-temporal Epidemiology

journal homepage: www.elsevier.com/locate/sste

Original Research

Dynamics of dengue disease with human and vector mobility

Murali Krishna Enduri*, Shivakumar Jolad

Indian Institute of Technology Gandhinagar, Gandhinagar, Gujarat 380005, India

ARTICLE INFO

Article history:
Received 21 February 2017
Revised 30 October 2017
Accepted 3 March 2018
Available online 10 March 2018

Keywords:
Dengue
Vector borne diseases
Epidemics
Cellular automata
Human mobility
Reaction–diffusion

ABSTRACT

Dengue is a vector borne disease transmitted to humans by *Aedes aegypti* mosquitoes carrying virus of different serotypes. Dengue exhibits complex spatial and temporal dynamics, influenced by various biological, human and environmental factors. In this work, we study the dengue spread for a single serotype (DENV-1) including statistical models of human mobility with exponential step length distribution, by using reaction–diffusion equations and Stochastic Cellular Automata (SCA) approach. We analyze the spatial and temporal spreading of the disease using parameters from field studies. We choose mosquito density data from Ahmedabad city as a proxy for climate data in our SCA model. We find an interesting result that although human mobility makes the infection spread faster, there is an apparent early suppression of the epidemic compared to immobile humans. The disease extinction time is lesser when human mobility is included.

1. Introduction

Dengue fever (DF) is a vector borne disease widely prevalent in tropical and subtropical regions in about 100 countries worldwide. The World Health Organization (WHO) reports that over 3.9 billion people, in 128 countries, are at risk of infection with dengue viruses (Brady et al., 2012), and an estimated 390 million dengue infections occur per year (Bhatt et al., 2013; WHO, 2017a). Dengue is transmitted to humans mainly through *Ae. aegypti* female mosquito bites carrying dengue virus (Nishiura, 2006). Dengue fever (DF), dengue hemorrhagic fever (DHF) and dengue shock syndrome (DSS) are different forms of dengue infection, caused by five serotypes of dengue virus, commonly known DENV:1-4 (WHO, 2017a) and the recently discovered DENV-5 (Mustafa et al., 2015). The people who recover from one serotype can become permanently immune to it, but may not be immune to other serotypes. Dengue is becoming a major public health concern in various South Asian and Latin American countries. Many dengue infections may not produce severe symptoms, thereby evading early detection. Vaccine for dengue serotypes has been under development and clinical trials for some years. Recently live tetravalent dengue vaccine CYD-TDV has completed Phase III trials and registered for use in individuals with 9–45 years in some endemic areas (Guy et al., 2011), (WHO, 2017b). It is believed that any future dengue vaccination is imperfect (Bhamarapravati and Sutee, 2000), and may not offer protection against all serotypes. The most effective way to prevent dengue outbreak is to devise vector control strategies and minimize vector–human transmission. A sound understanding of the spatial and temporal dynamics of the dengue can help in devising strategies for containing the spread urban populations.

Numerous human, biological, social and environmental factors affect the transmission of dengue (de Freitas et al., 2011), (Adams and Boots, 2010; Kuno, 1995). Several mathematical models have been proposed (see Andraud et al., 2012; Derouich and Boutayeb, 2006; Nishiura, 2006 for reviews) for studying the dengue. Many of these are the

* Corresponding author.
E-mail addresses: endurimuralikrishna@iitgn.ac.in (M.K. Enduri), shiva.jolad@iitgn.ac.in (S. Jolad).

https://doi.org/10.1016/j.sste.2018.03.001
1877-5845/

compartmental ordinary differential equation (ODE) models (Anderson and May, 1991), (Bailey et al., 1975), which divide the human population into Susceptible, Exposed, Infected, and Recovered (SEIR) groups; and vectors into Susceptible, Exposed, Infected (SEI) groups (Newton and Reiter, 1992), and studying their temporal dynamics. These ODE models are essentially mean field models which neglect the spatial patterns of the spread of dengue, which makes it unsuitable for studying the mobility effects on the spread of diseases. Attempts at spatial modeling of dengue includes those based on spatial data mapping and statistical analysis (Bhandari et al., 2008; Bohra and Andrianasolo, 2001; Peterson et al., 2005; Rotela et al., 2007), reaction–diffusion partial differential equation (PDE) with vector or larval mobility (Maidana and Yang, 2008; Tran and Raffy, 2006), Individual Based Models (IBM) on a grid (Barmak et al., 2011; Bian, 2004; Karl et al., 2014; Otero et al., 2011; 2008) including Cellular Automata approach with vector mobility and models of human mobility (de Castro Medeiros et al., 2011; Santos et al., 2009).

Human mobility, especially of the infected individuals can create multiple dengue waves resulting in substantial deviation from mean field results. However, the current approaches to study dengue spreading with human mobility have been restricted to simple methods such as movement with fixed step size, introducing a global field altering transition probabilities (de Castro Medeiros et al., 2011; Santos et al., 2009) and meta-population models (Adams and Kapan, 2009; Colizza and Vespignani, 2007; 2008; Stolerman et al., 2015). It has been studied at multiple scales (Balcan et al., 2009) such as house to house mobility (Stoddard et al., 2013), time of the day dependent mobility parameters (Karl et al., 2014), rural–urban daily commuters (Mpolya et al., 2014), dengue transmission and social ties dependent mobility (Reiner et al., 2014), and dengue spread across countries (Wichmann and Jelinek, 2004). In this work, we first report the results of SEIR-SEI reaction–diffusion PDE model with diffusive human mobility as a reference, and then include realistic models of human mobility patterns using *Stochastic Cellular Automata* (SCA) approach (closely following de Castro Medeiros et al., 2011). Mobility patterns are derived from statistical studies of human movements observed through the circulation of currency notes, tracking of phone calls through cellular towers, and location based social networks such as Foursquare. These works have shown varied patterns such as Lévy flight (Brockmann and Hufnagel, 2007; Brockmann et al., 2006), truncated Lévy flight (González et al., 2008), exponential distribution in intra urban movements (Liang et al., 2013 and Noulas et al., 2012). The differences arise possibly due to the difference in scale and resolution of study (large distance, intra city movements, mobile tower coverage etc.) and the methodology used. Dengue is endemic in densely populated tropical regions, typically in urban areas (Pongsumpun et al., 2008), although recently many studies on dengue in rural areas can also be found (Pérez-Castro et al., 2016; Reller et al., 2016). Here we focus on the dengue spread within an urban area and use exponential tail (Liang et al., 2013) distribution for studying human mobility affects on spread of dengue.

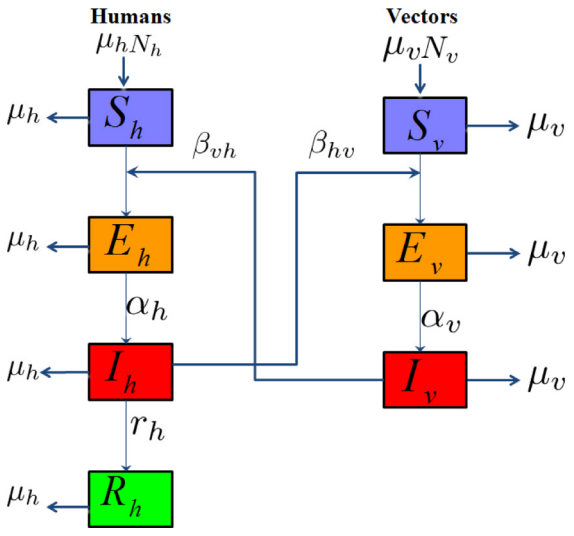

Fig. 1. SEIR-SEI compartmental model of human–vector interactions. Here μ_h, μ_v represent the human and vector mortality, $\beta_{hv}(\beta_{vh})$ represent the human (vector) to vector (human) transmission rate, $\alpha_h(\alpha_v)$ is the exposed to infection rate, r_h is the recovery rate in humans, and $N_h(N_v)$ is the total number of humans (vectors) involved in the dengue dynamics.

2. Model formulation

In this study, we use the standard compartmental model to divide the humans into SEIR and vector population into SEI groups (see Andraud et al., 2012; Nishiura, 2006 for review). Only infected vectors and infected humans can transmit the dengue virus to susceptible population (See Fig. 1 for illustration). Exposed population is infected with the virus but are *not infectious* (i.e. they cannot transmit the dengue virus). In Fig. 1, we show the flow diagram of SEIR-SEI model. The temporal evolution of the corresponding ordinary differential equations, their stationary states and stability conditions have been investigated and reported in many works (see for eg: Nishiura, 2006; Pongsumpun et al., 2008). In the next section, we focus on the spatial approaches to modeling dengue based on reaction diffusion equations.

2.1. Reaction–diffusion approach

In vector borne diseases, spatial spreading is possible only when there is mobility of vectors, humans or both. Vectors, especially *Ae. aegypti* rarely fly long distances by itself, and hence their mobility can be modeled a diffusion process (Maidana and Yang, 2008; Tran and Raffy, 2006). Their long distance mobility requires external drivers such as wind, vehicles, ships (Otero et al., 2008) and will not be considered here. Human mobility is more complex to analyze as multiple factors like population density, transportation networks, distribution of economic centers, urbanization pattern etc. However, these complex patterns can be summarized through statistical means by studying distributions like step length (Brockmann et al., 2006). A detailed discussions will be provided in Section 2.2.2.

Table 1
Table of parameters reaction–diffusion model (see Eq. 1 and 2) (Pongsumpun et al., 2008).

Parameter	Description	Value
μ_h	Death rate of humans	0.0000391 per day
μ_v	Death rate of vectors	0.07142 per day
β_{hv}	Infection rate from human to vector	0.00392 per day
β_{vh}	Infection rate from vector to human	0.0245 per day
r_h	Recovery rate of human population	0.07142 per day
α_h	Rate at which exposed human change to be infected human	0.2 per day
α_v	Rate at which exposed vector change to be infected vector	0.1 per day
D_v	Diffusion coefficient	0.2 cells per day

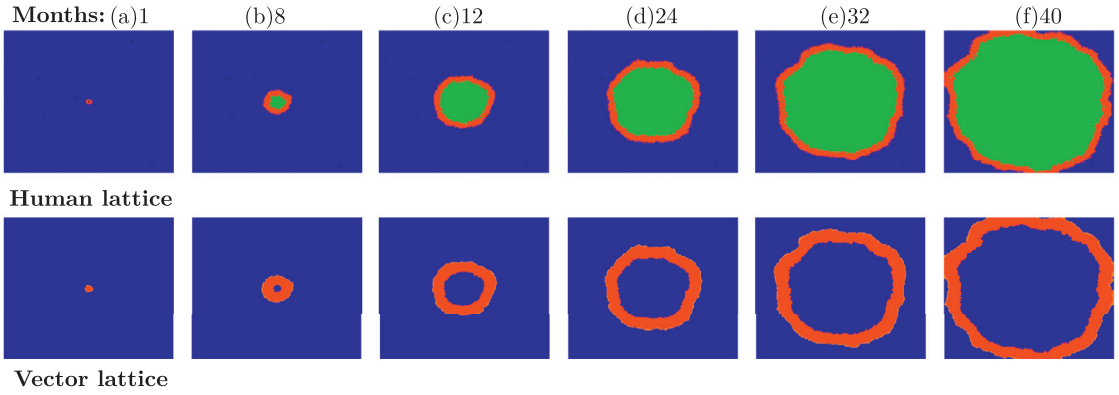

Fig. 2. Spatial temporal spread of dengue with reaction–diffusion equations with only vector mobility. Grid size is 500×500, $D_h = 0$. The upper row corresponds to human grid and the bottom row to vector grid. coloring scheme depend on the density of S(blue)-E(orange)-I(red)-R(green) and it is described in Section 2.1. (For interpretation of the references to color in this figure legend, the reader is referred to the web version of this article).

Reaction–diffusion (RD) equations are formed by adding diffusion terms to the reaction equations of the compartmental ODEs. Here, we model human mobility as a diffusive process and try to understand how the relative strengths of diffusion coefficients D_h/D_v affect the spatio-temporal spread of dengue. The RD equations for the humans in stages $\{S, E, I, R\}$ are given by:

$$\begin{aligned}
\frac{\partial s_h}{\partial t} &= D_h \nabla^2 s_h + \mu_h n_h - \beta_{vh} s_h i_v - \mu_h s_h \\
\frac{\partial e_h}{\partial t} &= D_h \nabla^2 e_h + \beta_{vh} s_h i_v - \alpha_h e_h - \mu_h e_h \\
\frac{\partial i_h}{\partial t} &= D_h \nabla^2 i_h + \alpha_h e_h - r i_h - \mu_h i_h \\
\frac{\partial r_h}{\partial t} &= D_h \nabla^2 r_h + r i_h - \mu_h r_h. \qquad (1)
\end{aligned}$$

The RD equations for the vectors in $\{S, E, I\}$ stages are given by:

$$\begin{aligned}
\frac{\partial s_v}{\partial t} &= D_v \nabla^2 s_v + \mu_v n_v - \beta_{hv} s_v i_h - \mu_v s_v \\
\frac{\partial e_v}{\partial t} &= D_v \nabla^2 e_v + \beta_{hv} s_v i_h - \alpha_v e_v - \mu_v e_v \\
\frac{\partial i_v}{\partial t} &= D_v \nabla^2 i_v + \alpha_v e_v - r i_h - \mu_v i_v, \qquad (2)
\end{aligned}$$

where $\{s, e, i, r\}$ represents the densities of humans and vectors in different compartmental stages, and $n_h = s_h + e_h + i_h + r_h$, $n_v = s_v + e_v + i_v$. Here μ_h, μ_v represent human and vector mortality (death) rates; β_{vh}, β_{hv} represent the vector to human and human to vector infection rates; α_h, α_v are the transition rates from exposed to infected states in humans and vectors; r is the recovery rate. The diffusion term $\nabla^2 = \frac{\partial^2}{\partial x^2} + \frac{\partial^2}{\partial y^2}$ is the 2D Laplacian operator. The above equations assume that the total population of humans and vectors is conserved. The death rate for humans (about 1/(75 yrs)) is much lower than that of vectors (about 1/14 days), hence the dynamical time scales vary widely. All the parameter values are shown in Table 1.

For the simulations we choose a 500×500 with Neumann boundary conditions. The spatial spread of dengue in humans and vectors with immobile humans ($D_h = 0$) are shown at various intervals in Fig. 2. The top (bottom) row shows the density of humans (vectors) in various stages of the disease. Initially (at $t = 0$), all humans are susceptible and all vectors, except the ones at the center are susceptible. Only the central cell vectors are initially infected with dengue. The coloring scheme for cells in the spatial grid are chosen according to the following rules: If the susceptible (recovered) density exceeds 0.5, the cell color is blue (green), or if the infected (exposed) density exceeds 0.25, it is painted red (orange).

The overall pattern of the dengue spread appears like a circular wave spreading outwards. This is due to the assumption of homogeneous and isotropic distribution of population, and diffusion constants being same in all directions. We observe that infection in the vector grid spreads faster than the human grid. We should note that the death rate of vectors is much higher than that of humans, but

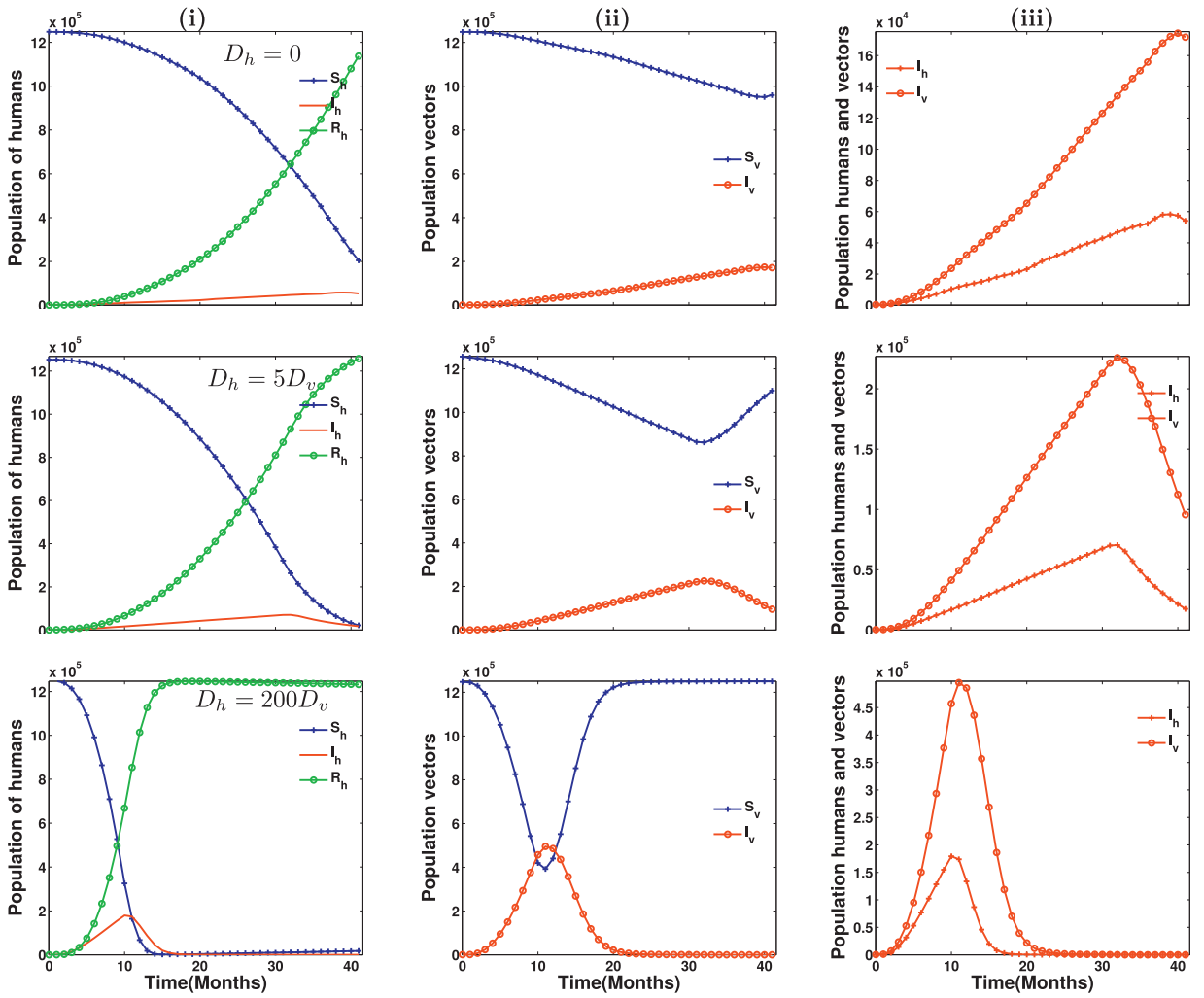

Fig. 3. Temporal dynamics of dengue reaction–diffusion model described in Eqs. (1) and (2). Columns: (i) SIR for humans, (ii) S-I for vectors (iii) Infected humans and vectors. Rows: diffusion rates 1) $D_h = 0$ 2) $D_h = 5D_v$ 3) $D_h = 200D_v$, with $D_v = 0.2$.

the incubation period is longer in vectors than humans ($\alpha_h > \alpha_v$). Hence we can observe the exposed vector population as a faint orange ring leading the infection.

The temporal variations of humans and vectors in different disease states for $D_h = \{0,\ 5D_v,\ 200D_v\}$ are shown in Fig. 3. The top row corresponds to immobile humans ($D_h = 0$). It exhibits typical SEI behavior up to 40 months. Afterwards the wave hits boundary (see Fig. 2f), halts the infection spread and everyone recovers. In the middle and bottom panel, we set human mobility to be same or higher order than the vectors by choosing $D_h = 5D_v$ and $D_h = 200D_v$ respectively, although we have tested for many other values of diffusion of constants. In all the cases, results showed a monotonic trend of infection suppression ($I_h(t) \to 0$, $R_h(t) \to S_h(0)$). Changing grid size only modified the time scale of suppression, and did not affect the main conclusions. Comparing these rows, we clearly see that the inclusion of human mobility causes early raise in the infected and then decline, as wave hits the boundary and infected recovers after the incubation period. This makes it appear that in the long run, human mobility suppresses infections compared to the immobile case.

2.2. Stochastic cellular automata

In Cellular Automata, space is divided into discrete grid and a finite state machine is assumed to operate at each grid point. At every time step, each cell is in one of the finite set of possible states. The transition probabilities depend only on the present state of the cell and its neighbors (Sarkar, 2000). This formalism can be modified to have agents placed in a cell (whose number can vary), who can change their states according to some specified rules. In this Stochastic Cellular Automata (SCA), agents can also be mobile.

We model the spatial dynamics of dengue using the SCA formalism by placing human and vector “agents” on two overlapping lattices and different disease states of these agents (de Castro Medeiros et al., 2011). We impose transition probabilities between the disease states based

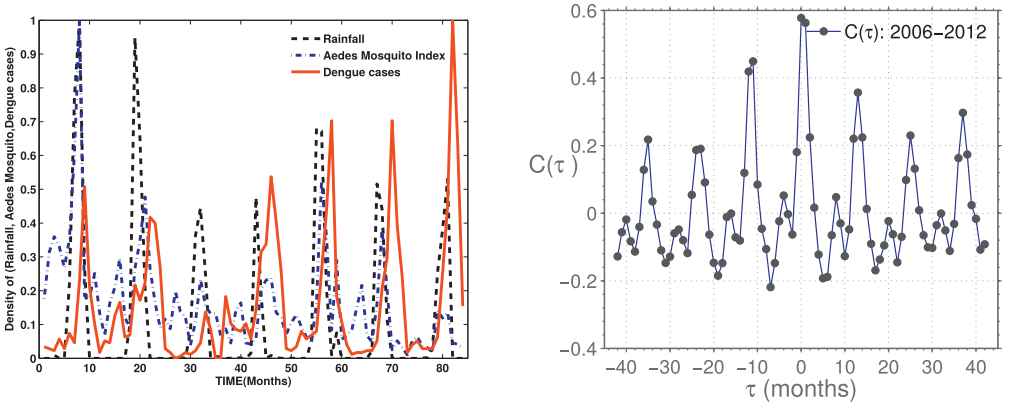

Fig. 4. (a) *Ae. aegypti* mosquito population and rainfall in Ahmedabad from 2006 to 2012 (source: Ahmedabad Municipal Corporation) (b) Corresponding cross correlation of rainfall and mosquito density.

Table 2
Value of parameters for stochastic cellular automata simulations.

Parameter	Description	Values
τ_{hE}	The duration for exposed human to become Infected	Uniform distribution: 4–7 days (Halstead, 2008)
τ_{vE}	Infected vectors incubation period	Uniform distribution: 8–12 days (Gubler et al., 2001; WHO, 2017a)
f_r	Maximum flight range of vectors	5 cells (25 m) (Kuno, 1995)
B_r	Biting rate of vectors	0–2/day (de Castro Medeiros et al., 2011)
β_{hv}, β_{vh}	Human to vector and vector to human transmission rates	{0.1, 0.15, 0.3, 0.9}

on field studies. For vectors we impose diffusive pattern, and for humans we use the exponential distribution of step length as described before. Climatic factors such as rainfall and temperature strongly affect the vector population. We have used mosquito density data of Ahmedabad city in mid-western India (with population of about 6 million) from 2006 to 2012 as proxy for climatic factors, as Aedes population shows strong correlation with rainfall (see Fig. 4), and it is a proximate determinant of dengue spreading. A detailed spectral analysis of dengue with climatic variables for Ahmedabad city has been reported recently by the authors Enduri and Jolad (2017).

Our primary focus though will be on understanding how mobility factors affect the spatio-temporal pattern of dengue. We choose the human (H) and vector (V) lattice to be of the same size. Each cell H_{ij} of human layer can have multiple agents (humans) in different disease states {S,E,I,R}, which can change with time. For example consider a cell H_{23} with 5 humans with {3S, 2E, 0I, 0R}. In the next time step, it can be {2S, 2E, 1I, 0R}. Similarly, in vector cell, mosquitoes can have states {S,E,I}, which can change with time. Throughout our simulations we take each time step to be one day. In Table 2, we summarize the main parameters used in our SCA simulations.

2.2.1. Vector population and mobility

In each cell of the vector lattice V_{ij}, mosquitoes are distributed according to the Poisson distribution $\mathcal{P}(\lambda_v)$, where λ_v is the average density of the *Ae. aegypti* mosquitoes in the cell. We use the periodic (monthly) data, denoted by $\{N_{m_1}, N_{m_2}, \ldots N_{m_n}\}$, on the *Aedes* mosquito density (Total knockout density measured by trapping mosquitoes in a room) available for Ahmedabad city in India from 2006 to 2012 (plotted in Fig. 4(a)) for simulations. The vector population is strongly correlated with the climatic factor, especially rainfall. The recorded dengue cases in Ahmedabad from 2006 to 2012 also plotted for comparison, although we should caution the reader that dengue cases in India are massively under reported (Kakkar, 2012). A recent detailed study reveals that the actual cases are estimated to be more than 5.78 million between 2006 and 2012 (Harris , New York Times; Shepard et al., 2014) in India, against the 28,000 reported cases (NCVRB, 2013). In Fig. 4(b) we show correlation of *Aedes* density with the rainfall during the same period. We observe peaks at periodic intervals, with the dominant one at multiples of 12 months. At the start of the simulation, in each cell the mean occupation is assumed to be $\lambda_v = N_m$, the measured average per room density of mosquitoes. To interpolate between the monthly data, we assume an exponential growth $n(t) = n(t_0)e^{r(t-t_0)}$ between month m_k and m_{k+1}, with growth rate $r = \frac{1}{30}\ln(N_{m_{k+1}}/N_{m_k})$, $n(t_0) = N_{m_k}$ and $t_0 \le t < t_0 + 30$. We denote the population in each cell from simulations be $n_s(t)$ and assign new births/deaths depending whether $\delta n = n(t) - n_s(t)$ is positive or negative. Although vertical transmission of dengue virus from mother to newborn mosquitoes is recorded, studies have shown that it does not affect long term virus persistence, due to low vertical infection inefficiencies (Adams and Boots, 2010). Hence we set the new born mosquitoes to be *susceptible*. If $\delta n > 0$, we generate new susceptible mosquitoes with Poisson distribution $\mathcal{P}(\delta n)$. If $\delta n < 0$, we calculate a random number $m = \mathcal{P}(-\delta n)$ and kill them in that cell.

Vector mortality: *Ae. aegypti*'s life span is short with average of 22 days and maximum of 45 days (de Freitas et al., 2011). Its death rate is not significantly affected by

whether it is carrying the dengue virus or not. Here we set the vector mortality rate to be constant μ_v per day.

Vector mobility: *Aedes* mosquito moves in small steps and rarely flies long distance (Tran and Raffy, 2006). The simplest description of its mobility can be done through hopping across Moore neighborhoods[1]. Since vectors may also reside in the same cell, we choose a simple model where at each time step 50% of the mosquitoes decide to move out of the cell. For the remaining mosquitoes the probability of hopping to a Moore neighborhood of range r is chosen to be $1/2^r$, with $r = 1, 2, \ldots, \infty$. Within this range, the probability of choosing any cell is uniform: $p = 1/((2r+1)^2 - 1)$. If we take a to be the width of each cell, the average distance along sides is $a\sum_{r=1}^{\infty} r/2^r = 2a$ (flight range of $f_r = 25m$), and along the diagonal is $2a\sqrt{2}$.

2.2.2. Humans lattice and mobility

In each cell, human occupation is chosen to be Poisson distribution $\mathcal{P}(\lambda)$ with mean $\lambda = 5$. The birth rate is balanced with the death rate to keep the population constant. Human mortality rate (1/70 yrs) is much smaller to compared to the vector and hence does not account for significant deaths during the simulation time. We also assume that the death rate due to dengue is zero as is the case DENV-1 infections.

Human mobility is primarily responsible for carrying communicable diseases to large distances, both within the city and across the cities and countries (Belik et al., 2011; Wichmann and Jelinek, 2004). Vector borne diseases can be spread by both human and vector mobility. A recent study with smaller population on 20×20 blocks, with a network based link length distribution following Lévy flight pattern shows that human mobility strongly enhances the infection dispersal in vector borne diseases (Barmak et al., 2011). Typically human mobility causes the virus to carry disease across different regions in much shorter time period than the vectors. The mobility of infected humans or vectors can create multiple waves of diseases at different locations. In SIR/SEIR model, mobility can also lead to depletion of infected in a particular region and hence local reduction in the transmission rates. Such competing forces call for a careful study of the mobility effects on the spread of vector borne diseases.

Many factors influence mobility within a city such as population density, transportation networks, traffic patterns and varying economic activity in different localities (home, work, school, shops, hospitals etc.). Modeling spatial human mobility in cities (especially in India) in the absence of credible data is a daunting task. Several ingenious methods have been used in the past to study the statistical patterns of human mobility. Tracking of currency notes yielded a scale free Lévy flight pattern (Brockmann et al., 2006) $P(\Delta r) \sim (\Delta r)^{-(1+\beta)}$ across large scale. Later, a study based on the trajectory of 100,000 anonymised mobile phone users (González et al., 2008) in US showed that the step length distribution behaves like a truncated Lévy flight $P(\delta r) = \frac{A}{(\delta r + \delta r_0)^{\beta}} \exp(-\delta r/\kappa)$.

[1] It consists of cells in a square neighborhood at an edge cell distance of r from the center. There are $(2r+1)^2$ cells in such a ring (Sarkar, 2000).

The advantage of these methods is that statistical patterns are robust and does not critically depend on the variations in transportation networks or population density. Dengue is reaches epidemic state mainly in urban areas where the population density is high (Pongsumpun et al., 2008) and mobility within the city spreads the disease faster. Study of intra-urban mobility received special attention in the recent years. Liang et al. (2013) have produced a strong evidence of exponential distribution in intra-urban movements. It is supported by a recent study by Noulas et al., where they explore intra city movements using location data by social networking site Foursquare (Noulas et al., 2012). In this work, we choose exponential step length model $P(\Delta r) = \lambda e^{-\lambda \Delta r}$ for studying human mobility. Liang et al. found the mobility exponent λ is not universal, and varies like 0.08 km^{-1} in Los Angeles to 0.22 km^{-1} in Beijing (Liang et al., 2013). In our model world, we choose the distribution in terms of characteristic step length w to be

$$P(l) = \frac{1}{w} e^{-l/w}, \tag{3}$$

where l is step length scaled to the lattice size.

In this work, we restrict the mobility to S, E and R population. Infected are assumed to be immobile which may not be true in all cases, but it simplifies our model description. With a 50% probability of S, E or R type people move from their current cell following above distribution (our simulations show that even if we relax this assumption, main result does not vary significantly). Once a person decides to move, a random number following exponential distribution (as in Eq. 3) is drawn and step length is determined. The angle is chosen from a uniform distribution $U(0, 2\pi)$. The cell which contains the location $(\delta r, \theta)$ from the current point is chosen as the destination cell. If the range is outside the SCA boundary, periodic boundary conditions bring the person back into the SCA world. This ensures that net migration in and out of SCA is zero.

2.2.3. Interactions between humans and vectors

Human–vector and vector–human interaction happens mainly through mosquito bites. We have set the maximum biting rate to two and assumed that the probability of {0, 1, 2} bites are {1/4, 1/2, 1/4} respectively. In each cell, an *Ae. aegypti* mosquito (of any type S,E or I) randomly selects a human to bite and after each bite, the vector stays in the same cell or follows the vector mobility pattern described before. The dengue virus is transmitted from human to vector (or vice-versa) when an infected vector I_v bites a human in a susceptible state (S_h) or an infected human I_h gets bitten by a susceptible mosquito S_v with rate β_{hv} (β_{vh}). Our β_{hv} values were chosen so that it spans the range of disease suppression and endemic states . The epidemic threshold falls at $\beta_{hv} = 0.3$. We have taken two values below the threshold $\beta_{hv} = \{0.1, 0.15\}$ and two values above the threshold $\beta_{hv} = \{0.3, 0.9\}$.

3. Results

We have studied dengue spread for both immobile and mobile humans. Our analysis is primarily focused on tem-

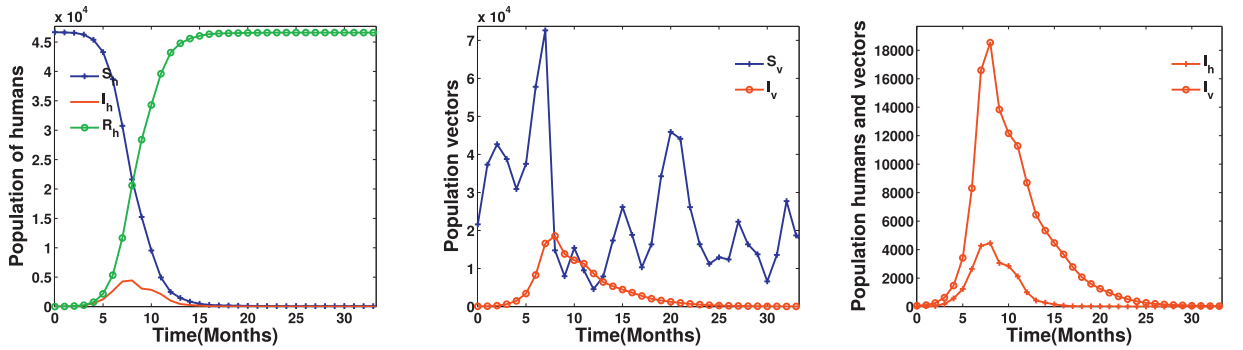

Fig. 5. Temporal dynamics of dengue from stochastic Cellular Automata ($\beta_{hv} = 0.9$) (a) susceptible, infected and recovered humans (b) susceptible and infected vectors (c) infected humans and infected vectors.

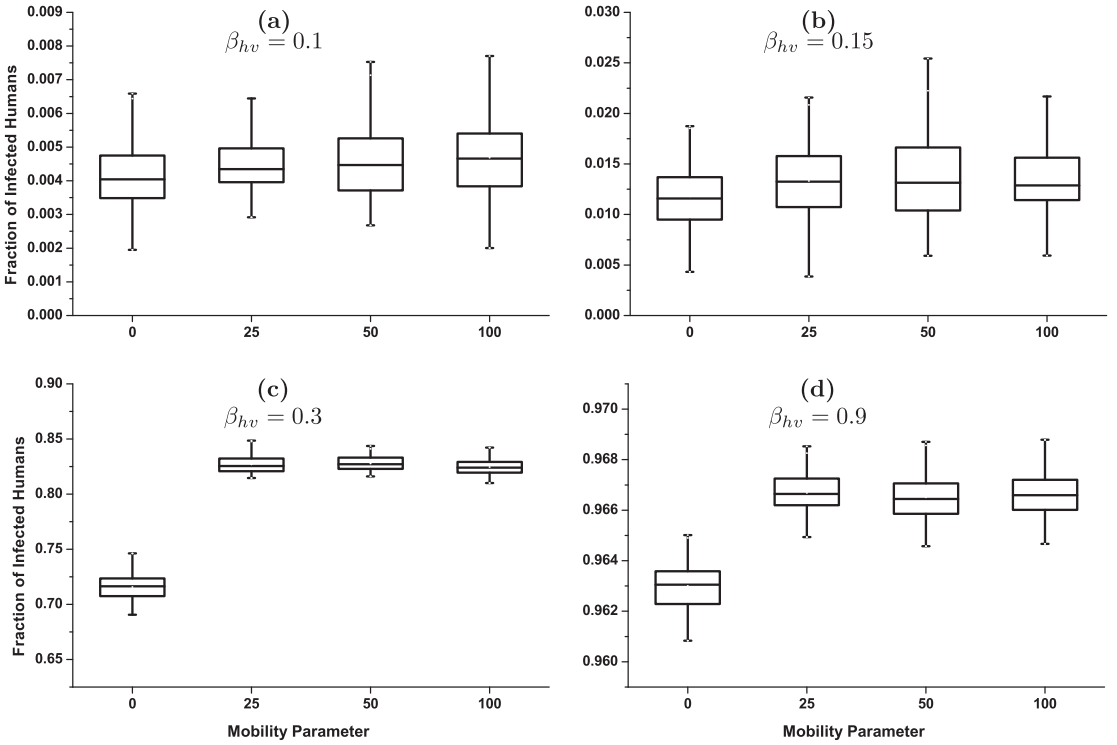

Fig. 6. Box plots of fraction of infected at the end of simulation with different exponential mobility scale ($P(l) = 1/we^{-l/w}$) $w = \{0, 25, 50, 100\}$ and different infection rate (a) $\beta_{hv} = 0.1$ (b) $\beta_{hv} = 0.15$ (c) $\beta_{hv} = 0.3$ (d) $\beta_{hv} = 0.9$. The difference in scale across panels is used for clarity in illustrating the result.

poral dynamics of dengue. The process of modeling human mobility has been described in Section 2.2. Susceptible people can get infected when they move to cells where the vectors in the neighborhood cells are infected. For statistical validation, we choose a lattice 100×100 and an average human occupancy of 5 agents per cell, for all the infection rates and mobility parameters described before. We repeat it 100 times with different random number seeds for statistical validation.

We first present the SEIR-SEI temporal dynamics for a particular infection rate. The temporal patterns of human and vector population, infected human and infected vector and SIR groups of humans are shown in Fig. 5. Here we observe that at any time, the fraction of infected is quite small when compared to susceptibles (panel a). But, over time large fraction of the population will be infected and move to recovery phase (as expected from SEIR dynamics, R monotonically increases in active phase if there are no deaths). Similar trend can be seen for vectors in panel b. On a closer look, (panel c), we see that both infected humans and infected vectors show substantial variations in time.

To compare the difference in dengue dynamics with and without human mobility, we computed several variables of interest such as (a) total infected population during the entire simulation (recovered at $t = t_f$) (b) disease extinction time (c) time at which infection peaks. In Fig. 6, we show the box plot of the fraction of total infected

Table 3
Recovered people (in thousands) at the end of simulation- 95% confidence interval about mean ($\bar{x} \pm 1.96\sigma/\sqrt{n_s}$) (Average population 46.6 thousand and number of simulation runs n_s=100).

β_{hv}	w=0	25	50	100
0.1	0.19 (0.18, 0.20)	0.21 (0.20, 0.22)	0.21 (0.20, 0.22)	0.21 (0.20, 0.22)
0.15	0.55 (0.52, 0.57)	0.62 (0.59, 0.65)	0.63 (0.59, 0.67)	0.63 (0.60, 0.66)
0.3	33.35 (33.21, 33.48)	38.54 (38.46, 38.62)	38.56 (38.49, 38.63)	38.41 (38.33, 38.48)
0.4	42.15 (42.09, 42.20)	43.54 (43.49, 43.60)	43.48 (43.43, 43.54)	43.38 (43.32, 43.45)
0.6	44.27 (44.22, 44.30)	45.02 (44.97, 45.06)	45.04 (44.99, 45.08)	45.07 (45.04, 45.11)
0.9	44.89 (44.85, 44.93)	45.00 (44.96, 45.04)	45.04 (45.01, 45.08)	45.02 (44.98, 45.06)

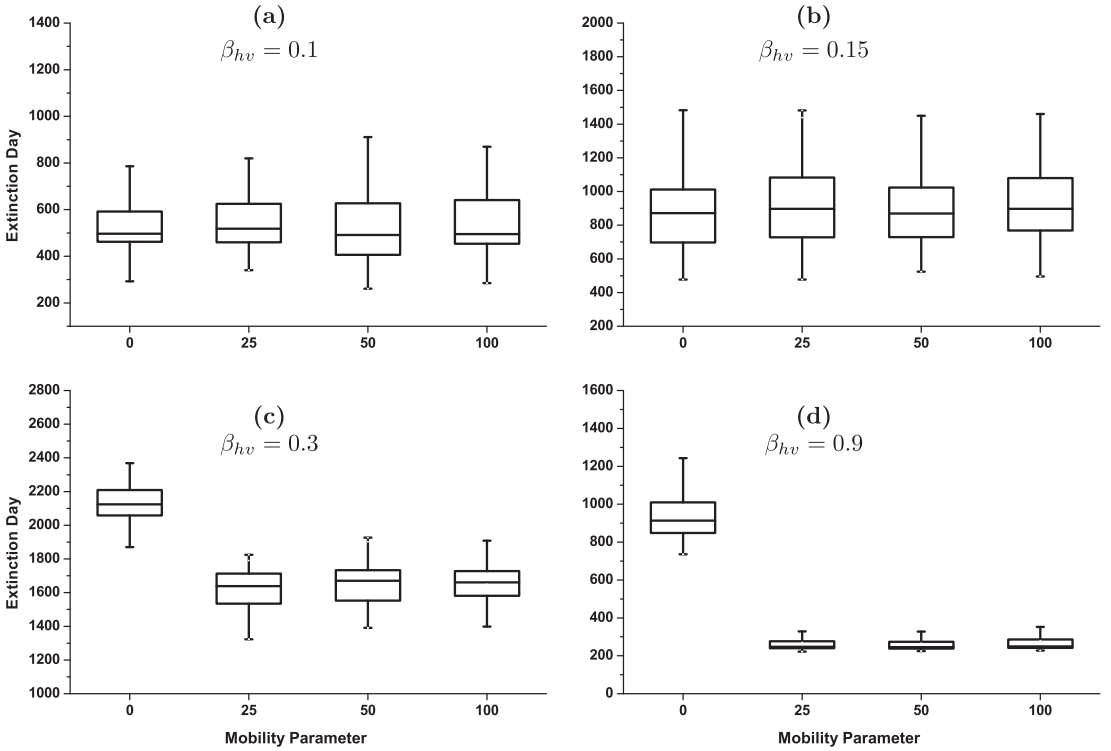

Fig. 7. Box plots of number of days for extinction with different exponential mobility scale $w = \{0, 25, 50, 100\}$ and different infection rate (a) $\beta_{hv} = 0.1$ (b) $\beta_{hv} = 0.15$ (c) $\beta_{hv} = 0.3$ (d) $\beta_{hv} = 0.9$. Note the difference in axis scale across panels.

population at the end of simulation ($R(t_f)/S(0)$) for different mobility parameters $w = \{0, 25, 50, 100\}$. The $w = 0$ represents immobile case. For low value of β_{hv} (< 0.15), we observe that infection dynamics is in inactive state. For higher β_{hv} (≥ 0.3), disease dynamics enters an active state with large proportion of population being infected. We can observe (in panel a and b) at low values of $\beta_{hv} = \{0.1, 0.15\}$ fraction of infection population is not more than 0.02% for any mobility (w). There is no statistical difference between mobile and immobile case and infection levels are fully suppressed. For $\beta_{hv} = \{0.3–0.9\}$ (in panel c and d) we can clearly distinguish between fraction of infected population when we include human mobility ($w = \{25, 50, 100\}$). For very high infection rates (say $\beta_{hv} = 0.9$), almost all people are infected, but still small difference is maintained for mobile and immobile cases (panel d). In Table 3, we have tabulated mean and 95%confidence interval of $R(t_f)$ for various w's and β's. We observe that in active state, confidence intervals with and without human mobility do not overlap.

Disease dynamics stops when there are no infected humans and vectors. In Fig. 7 we show the box plot of extinction time for different infection rates and mobility parameters. Panel a and b refers to the absorbing state, where no statistical difference is seen between with and without mobility cases. For the disease endemic state ($\beta \geq 0.3$), we see a surprising result that human mobility has caused disease to die down faster than the case without human mobility. This result is counter intuitive given that mobility causes greater number of infected people than immobile case (as in Fig. 6c and d), but we see disease extinction to be faster when we include mobility. Mobility causes secondary and tertiary waves of infection, who recover in short time and act as barricade for the spreading of primary epidemic wave. Mobility speeds up the infection spread as well as recovery driving the disease to

go extinct earlier. Reaction-diffusion studies in section II A support this finding, where inclusion of mobility (Fig. 3 second and third row, $D_h = 5D_v$, $200D_v$) caused early suppression of infection, but not before everyone has recovered.

4. Summary and outlook

Many authors have approached human mobility and spread of vectors borne diseases from multiple perspectives, looking primarily into how mobility exacerbates the disease spreading. In this we work we have focused our attention on dengue epidemic suppression time.

We have studied the spatio-temporal dynamics of transmission of dengue in human and vector population through reaction–diffusion and stochastic Cellular Automata (SCA) formalism. Though our simulations are spatial, we do not include spatial heterogeneities in human and vector density due to lack of data. We have divided human and vector population into SEIR-SEI compartments and distributed them on a bi-layer SCA lattice. Coupling between the lattices is through vector bites, which transmits the disease across the layers. Mobility of vectors and humans spread the disease both within and across their lattice. As inputs to the model, we have used parameters from field studies, and vector population data from the Ahmedabad city in India. We have imposed a statistical pattern of human mobility (exponential distribution) on the human lattice to understand how mobility affects the spread of vector borne diseases.

Our main work is to understand the effect of human mobility on dengue spreading has shown some surprising results. Movement of susceptible and exposed humans lead to an apparent suppression of the epidemic. Time of extinction of disease is lower when mobility is included, but leads to higher number of people infected during the dengue cycle. In particular, our work was restricted to densely populated city like Ahmedabad, where the reproduction number for dengue is high during monsoons (calculated in Enduri and Jolad, 2017). Mobility may have caused the disease to spread to much larger fraction of population than what is reported, but may largely be undetected because symptoms in many are mild and large cases are under reported (Kakkar, 2012). Since the spreading rate is fast, and people recover quickly, we get an apparent early suppression of disease.

In this work we have made several assumptions for simplifying simulations and analysis. Dengue is increasingly being reported in rural areas too, especially in India, and sparse attention is paid to ruralization of dengue fever. We have restricted the study to one city, and have neglected mobility across cities and rural–urban areas. Since the definitions of rural and urban areas is complex and vary from country to country, future studies in dengue should use population density as parameter rather than restricting to urban areas. We neglected spatial heterogeneities due to paucity of spatial data. In future, more realistic simulations on dengue in India should include data on population distribution within a city, presence of stagnant water bodies, and slum dwellings to account for spatial heterogeneities. Inclusion of environmental variables such as rainfall can serve as proxy water clogging and temperature which affects the breeding time of vectors. In this work, statistical patterns of human mobility has been taken from studies in US, UK and China. It is not clear (due to lack of literature), whether the same patterns hold good in developing countries such as India, where the current study focuses on. Mobility patterns are closely linked to transportation networks and traffic density. Inclusion of these factors, along with population density can give us more specific insights into how mobility affects spread of vector borne diseases in cities. We hope that the present work will motivate researchers to take up such studies in the future.

Acknowledgment

The authors would like to thank Vinod Reddy, Richard Koblenu, and Profs. Malavika Subramanyam, Bireswar Das, and Ravindra Amritkar for insightful discussions and suggestions. We specially thank Dr. V K Kohli, Assistant Entomologist Ahmedabad Municipal Corporation for providing us with data on dengue incidences and mosquitoes in Ahmedabad city.

References

Adams B, Boots M. How important is vertical transmission in mosquitoes for the persistence of dengue? Insights from a mathematical model.. Epidemics 2010;2(1):1–10. doi:10.1016/j.epidem.2010.01.001.

Adams B, Kapan DD. Man bites mosquito: understanding the contribution of human movement to vector-borne disease dynamics.. PloS One 2009;4(8):e6763. doi:10.1371/journal.pone.0006763.

Anderson RM, May RM, 1. Oxford university press Oxford; 1991.

Andraud M, Hens N, Marais C, Beutels P. Dynamic epidemiological models for dengue transmission: a systematic review of structural approaches.. PloS One 2012;7(11):e49085. doi:10.1371/journal.pone.0049085.

Bailey NT, et al. The mathematical theory of infectious diseases and its applications. Charles Griffin & Company Ltd, 5a Crendon Street, High Wycombe, Bucks HP13 6LE.; 1975.

Balcan D, Colizza V, Gonçalves B, Hu H, Ramasco JJ, Vespignani A. Multiscale mobility networks and the spatial spreading of infectious diseases. Proc Natl Acad Sci 2009;106(51):21484–9.

Barmak DH, Dorso CO, Otero M, Solari HG. Dengue epidemics and human mobility. Phys Rev E 2011;84(1):011901. doi:10.1103/PhysRevE.84.011901.

Belik V, Geisel T, Brockmann D. Natural human mobility patterns and spatial spread of infectious diseases. Phys Rev X 2011;1(1):011001.

Bhamarapravati N, Sutee Y. Live attenuated tetravalent dengue vaccine. Vaccine 2000;18:44–7.

Bhandari KP, Raju P, Sokhi BS. Application of gis modeling for dengue fever prone area based on socio-cultural and environmental factors–a case study of delhi city zone. Int Arch Photogramm Remote Sens Spat Inf Sci 2008;37:165–70.

Bhatt S, Gething PW, Brady OJ, Messina JP, Farlow AW, Moyes CL, Drake JM, Brownstein JS, Hoen AG, Sankoh O, Myers MF, George DB, Jaenisch T, Wint GRW, Simmons CP, Scott TW, Farrar JJ, Hay SI. The global distribution and burden of dengue. Nature 2013. doi:10.1038/nature12060.

Bian L. A conceptual framework for an individual-based spatially explicit epidemiological model. Environ Plann B 2004;31(3):381–96.

Bohra A, Andrianasolo H. Application of GIS in modelling of dengue risk based on socio-cultural data: case of Jalor, Rajasthan, India. Conference for remote imaging, sensing and processing, NUS; 2001. p. 5–9.

Brady OJ, Gething PW, Bhatt S, Messina JP, Brownstein JS, Hoen AG, Moyes CL, Farlow AW, Scott TW, Hay SI. Refining the global spatial limits of dengue virus transmission by evidence-based consensus. PLoS Neglect Trop Dis 2012;6(8):e1760.

Brockmann D, Hufnagel L. Front propagation in reaction-superdiffusion dynamics: taming lévy flights with fluctuations. Phys Rev Lett 2007;98(17):178301. doi:10.1103/PhysRevLett.98.178301.

Brockmann D, Hufnagel L, Geisel T. The scaling laws of human travel.. Nature 2006;439(7075). doi:10.1038/nature04292. 462–5
de Castro Medeiros LC, Castilho CAR, Braga C, de Souza WV, Regis L, Monteiro AMV. Modeling the dynamic transmission of dengue fever: investigating disease persistence. PLOS Neglect Trop Dis 2011;5(1):e942.
Colizza V, Vespignani A. Invasion threshold in heterogeneous metapopulation networks. Phys Rev Lett 2007;99(14):148701.
Colizza V, Vespignani A. Epidemic modeling in metapopulation systems with heterogeneous coupling pattern: theory and simulations. J Theoret Biol 2008;251(3):450–67.
Derouich M, Boutayeb A. Dengue fever: Mathematical modelling and computer simulation. Appl Math Comput 2006;177(2):528–44.
Enduri MK, Jolad S. Estimation of reproduction number and non stationary spectral analysis of dengue epidemic. Math Biosci 2017;288:140–8.
de Freitas RM, Koella J, de Oliveira RL. Lower survival rate, longevity and fecundity of aedes aegypti (diptera: Culicidae) females orally challenged with dengue virus serotype 2. Trans R Soc Trop Med Hyg 2011;105(8):452–8. doi:10.1016/j.trstmh.2011.05.006.
González MC, Hidalgo Ca, Barabási AL. Understanding individual human mobility patterns.. Nature 2008;453(7196). doi:10.1038/nature06958. 779–82
Gubler DJ, Reiter P, Ebi KL, Yap W, Nasci R, Patz JA. Climate variability and change in the united states: potential impacts on vector-and rodent-borne diseases.. Environ Health Perspect 2001;109(Suppl 2):223.
Guy B, Barrere B, Malinowski C, Saville M, Teyssou R, Lang J. From research to phase iii: preclinical, industrial and clinical development of the sanofi pasteur tetravalent dengue vaccine. Vaccine 2011;29(42):7229–41. doi:10.1016/j.vaccine.2011.06.094. The Development of Dengue Vaccines
Halstead SB. Dengue virus-mosquito interactions. Annu Rev Entomol 2008;53:273–91.
Harris (New York Times) G.. Study reassesses dengues impact in india. 2014. [Online; posted 7-October-2014].
Kakkar M. Dengue fever is massively under-reported in india, hampering our response. BMJ: Br Med J 2012;345.
Karl S, Halder N, Kelso JK, Ritchie SA, Milne GJ. A spatial simulation model for dengue virus infection in urban areas. BMC Infect Dis 2014;14(1):447.
Kuno G. Review of the factors modulating dengue transmission. Epidemiol Rev 1995;17(2):321–35.
Liang X, Zhao J, Dong L, Xu K. Unraveling the origin of exponential law in intra-urban human mobility. Sci Rep 2013;3.
Maidana NA, Yang HM. Describing the geographic spread of dengue disease by traveling waves.. Math Biosci 2008;215(1):64–77. doi:10.1016/j.mbs.2008.05.008.
Mpolya EA, Yashima K, Ohtsuki H, Sasaki A. Epidemic dynamics of a vector-borne disease on a villages-and-city star network with commuters. J Theoret Biol 2014;343:120–6.
Mustafa M, Rasotgi V, Jain S, Gupta V. Discovery of fifth serotype of dengue virus (denv-5): a new public health dilemma in dengue control. Med J Armed Forces India 2015;71(1):67–70.
NCVRB. Data from national vector borne diseases control program director general of health services. 2013.
Newton E, Reiter P. A model of the transmission of dengue fever with an evaluation of the impact of ultra-low volume (ulv) insecticide applications on dengue epidemics.. Am J Trop Med Hyg 1992;47(6):709–20.
Nishiura H. Mathematical and statistical analyses of the spread of dengue. Dengue Bull 2006;30:51–67.
Noulas A, Scellato S, Lambiotte R, Pontil M, Mascolo C. A tale of many cities: universal patterns in human urban mobility. PloS One 2012;7(5):e37027.
Otero M, Barmak DH, Dorso CO, Solari HG, Natiello MA. Modeling dengue outbreaks. Math Biosci 2011;232(2):87–95.
Otero M, Schweigmann N, Solari HG. A stochastic spatial dynamical model for Aedes aegypti.. Bull Math Biol 2008;70(5). doi:10.1007/s11538-008-9300-y. 1297–325
Pérez-Castro R, Castellanos JE, Olano VA, Matiz MI, Jaramillo JF, Vargas SL, Sarmiento DM, Stenström TA, Overgaard HJ. Detection of all four dengue serotypes in aedes aegypti female mosquitoes collected in a rural area in colombia. Memorias do Instituto Oswaldo Cruz 2016;111(4):233–40.
Peterson AT, Martínez-Campos C, Nakazawa Y, Martínez-Meyer E. Time-specific ecological niche modeling predicts spatial dynamics of vector insects and human dengue cases. Trans R Soc Trop Med Hyg 2005;99(9):647–55.
Pongsumpun P, Garcia Lopez D, Favier C, Torres L, Llosa J, Dubois Ma. Dynamics of dengue epidemics in urban contexts.. Trop Med Int Health: TM & IH 2008;13(9). doi:10.1111/j.1365-3156.2008.02124.x. 1180–7
Reiner RC, Stoddard ST, Scott TW. Socially structured human movement shapes dengue transmission despite the diffusive effect of mosquito dispersal. Epidemics 2014;6:30–6.
Reller ME, de Silva AM, Miles JJ, Jadi RS, Broadwater A, Walker K, Woods C, Mayorga O, Matute A. Unsuspected dengue as a cause of acute febrile illness in children and adults in western nicaragua. PLoS Neglect Trop Dis 2016;10(10):e0005026.
Rotela C, Fouque F, Lamfri M, Sabatier P, Introini V, Zaidenberg M, Scavuzzo C. Space–time analysis of the dengue spreading dynamics in the 2004 tartagal outbreak, northern argentina. Acta Trop 2007;103(1):1–13.
Santos L, Costa M, Pinho S, Andrade R, Barreto F, Teixeira M, Barreto M. Periodic forcing in a three-level cellular automata model for a vector–transmitted disease. Phys Rev E 2009;80(1):016102.
Sarkar P. A brief history of cellular automata. ACM Comput Surv (CSUR) 2000;32(1):80–107.
Shepard DS, Halasa Ya, Tyagi BK, Adhish SV, Nandan D, Karthiga KS, Chellaswamy V, Gaba M, Arora NK. Economic and disease burden of dengue illness in India. Am J Trop Med Hyg 2014. doi:10.4269/ajtmh.14-0002.
Stoddard ST, Forshey BM, Morrison AC, Paz-Soldan Va, Vazquez-Prokopec GM, Astete H, Reiner RC, Vilcarromero S, Elder JP, Halsey ES, Kochel TJ, Kitron U, Scott TW. House-to-house human movement drives dengue virus transmission.. Proc Natl Acad Sci USA 2013;110(3). doi:10.1073/pnas.1213349110. 994–9
Stolerman LM, Coombs D, Boatto S. Sir-network model and its application to dengue fever. SIAM J Appl Math 2015;75(6):2581–609.
Tran A, Raffy M. On the dynamics of dengue epidemics from large-scale information.. Theoret Popul Biol 2006;69(1):3–12. doi:10.1016/j.tpb.2005.06.008.
WHO. Dengue: fact sheets. 2017a.
WHO. Dengue vaccine research. 2017b.
Wichmann O, Jelinek T. Dengue in travelers: a review. J Travel Med 2004;11(3):161–70.